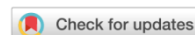




An Effort for Identifying Suitable Machining Range During Drilling of a Novel Al-Based Composite Using Electric Discharge Machine



Ankit Jain¹, Cheruku Sandesh Kumar^{1*} and Yogesh Shrivastava²

¹Amity University Rajasthan, Jaipur, India; ²Galgotias College of Engineering and Technology, Greater Noida, U.P., India

E-mail/Orcid Id:

AJ,  mittalankit.amity@gmail.com,  <https://orcid.org/0000-0002-2784-2633>; CSK,  sandeshkumar7@gmail.com;

YS,  yogeshshrivastava90@gmail.com,  <https://orcid.org/0000-0002-4037-2680>

Article History:

Received: 24th Oct., 2023

Accepted: 16th Dec., 2023

Published: 30th Dec., 2023

Keywords:

Drilling, EDM, MMC, Quality characteristics, RSM

How to cite this Article:

Ankit Jain, Cheruku Sandesh Kumar and Yogesh Shrivastava (2023). An Effort for Identifying Suitable Machining Range During Drilling of a Novel Al-Based Composite Using Electric Discharge Machine. *International Journal of Experimental Research and Review*, 36, 327-346.

DOI:

<https://doi.org/10.52756/ijerr.2023.v36.030>

Abstract: Various aluminium-based metal matrix composites (MMCs) have recently attracted significant interest and increased popularity. This is because of its' outstanding mechanical properties, which makes it a very popular material since it has various applications in industries that need strong yet lightweight materials with high strength. Researchers have made great progress in the mechanical properties of Al-based composites. In any case, it becomes imperative to improve the mechanical characteristics of the given material on demand. The current work aims at producing these aluminium-based MMC and, subsequently, precise machined EDM. It is an uncommon machining process typically known to produce tough materials of any arbitrary geometry. EDM is a technique that involves the fine-tuning of the electrode material, pulse length, and pulse current to yield the best results without causing much damage to the workpiece and maintaining its mechanical strength. Lastly, the research comprises an elaborate discussion on the optimum process parameters and experimental results about the effective manufacture of superior strength aluminium-based composites as well as their accurate electro-discharge machining. These results provide valuable information on making and machine metals for various technical uses across construction, mechanical engineering and electronics manufacturing industries.

Introduction

The advent of metal matrix composites-based aluminium has proven highly effective and applicable due to its unique mechanical properties. There are various forms of manufacturing techniques and settings which have proved fruitful in making aluminium-based MMC with high efficiency and greater strength. Ravikumar et al. (2018) explored the influence of distinct reinforcement elements on the mechanical properties of aluminium MMCs. They compared steel reinforcement in stir-casting (Al and Mg) with ceramic powders (SiC and Al₂O₃). This resulted in higher tensile strength of the composite reinforced by SiC, qualifying it for aeronautic structural applications. The powder metallurgy process has been done intensively to produce aluminium-based MMC with superior properties. In a broad-based study by Nath and

Madhu (2021) and Zamani et al. (2021), researchers investigated the influence various processing factors had on the mechanical properties of Al/SiC composites.

The variables included the sintering temperature, holding period, and rate at which cooling took place, to ensure even distribution without voids and attained high PVF. This improved toughness, wear resistance and hardness tremendously. The in-situ synthesis technique represents the suitable method of manufacturing for strengthening interphase adhesion at the aluminium/reinforcement interface. For example, Lu et al. (2020) researched the in-situ growth of TiC particles with the aluminium matrix in their study. The study revealed that the addition of TiC reduced grains in heat treatment and thus strengthened the mechanical properties of the composite. The right way to select



production process and reinforcement materials for achieving the proper material performance is just one of the processes in this process. Another process involves optimization of processing parameters. A study by Zhu et al. (2020) looked into the relationship between the stir casting speeds and the microstructure and mechanical properties of Al/SiC composites. It was discovered that an appropriate stirring rate ensured the homogenous distribution of SiC particles, leading to an increase in hardness and tensile strength. Much of the assessment of the quality and characteristics of fabricated Al-based MMC is through characterization techniques. Muni et al. (2022) investigated microstructure and phase composition of PM-based Al/Al₂O₃ composites applying XRD and SEM. Characterization showed that production was successful and proved the mechanical strength of the composites. The microstructure analysis also showed uniform distribution of aluminium oxide particles. The researchers used a variety of reinforcing materials, such as Al-based MMCs with superior mechanical properties in their study by Yadav et al. (2021). By using powder metallurgy, they studied the effects of adding SiC/CNT in combination as reinforcements. The synergistic improvement in the tensile strength and the hardness were attributed to the complementary strengthening mechanisms by SiC and CNTs. The present study shows how the incorporation of hybrid strength composites could alter mechanical properties of the aluminium-based MMC's for specific applications. Recently, experts have focused on environmental issues in which they try to minimize the impact by practising green manufacturing.

Santiago et al. (2022) discussed the importance of using recycled aluminium scraps as a matrix material for making aluminium-based metal matrix composites. They applied stir casting to include various reinforcement materials while considering the mechanics of the composite. These indicated that using the recovered or recycled aluminium in composite manufacture gave out products similar in quality for utilization as reusable structural elements in "green" engineered systems and also saved the manufacturing cost. They have attracted attention for their sophisticated additive manufacturing processes that are able to develop complex geometries – a notable departure from traditional manufacturing techniques. Weng et al. (2020), developed SLM-made aluminium MMCs containing Al₂O₃ reinforcements. This study aimed to determine how the improved mechanical properties are achieved in high density composite by augmenting the SLM process settings. This helps make high-quality aluminium based MMC products

in short time frames, specifically tailored for different use cases.

Many researches are focused on treatments for manufactured aluminium-MMCS surfaces to improve their performance reliability. Scientists also studied the effect of shot peening on the fatigue properties of PM-Al/SiC composites. When subjected to a 30-minute heat treatment at 500 deg F, the shot peening created high levels of compressive residual stress, which significantly prolonged the fatigue life and made it suitable for applications where higher fatigue resistance is mandatory. The precision machining of these types of hybrid composites has also been an important issue in addition to their productions. Many evidences showed, drilling of these kinds' materials always involved unexpected shifts in quality attributes. Several detailed research papers are about EDM drilling of metal matrix composite drills. Study results have enabled an understanding of how EDM on-time, off-time, distilled water pressure as well as the discharge current affect performance of high-strength aluminum-based MMCs during drilling. Several studies on the impact of these variables on hole taper and circularity, among other aspects of drilling, are available. To investigate the effect of pulse on-time and pulse off-time on the EDM drilling process, Kumar et al. (2018) conducted an investigation to assess the impact of pulse on-time and pulse off-time on the EDM drilling processes for Al/SiC MMCs. They changed the pulse on-time, $\mu\text{s/p}$ and pulse off-time, $\mu\text{s/p}$. The outcomes included shorter pulse-on and longer pulse-off periods, thus decreasing electrode wear and improving surface polishing. This shows that one should understand the characteristics of the discharge during EDM drilling and change the process parameters in favour of Al-based MMCs. Distilled water pressure (kg/cm^2): Another study was conducted by Nayak et al. (2022) investigating EDM drilling performances as a function of the pressure used in water distillate in Al/Al₂O₃ MMCs. They considered the effects of varying the water pressure on the heat-affected zone, hole quality, and material removal rate. The data showed that a high level of water pressure was more effective in a flushing process, which led to enhanced surface quality as well as a lesser hole angle. Discharge current is a key factor in EDM drilling because it affects how much energy goes into the spark and how fast the material is removed.

Sharma et al. (2023) investigated the influence of drill current on the drilling properties of P/M'12' made Al/SiC MMCs. Increasing the discharge current improved material removal rates but wore out electrodes and lowered circular holes. The circularity of such drilled

holes is a significant mark of the excellence and accuracy of these holes. Teng et al. (2018) studied the circularity (or hole entry and exit points) of holes drilled in the Al/CNT MMC samples fabricated with various combinations of pulse ON times, pulse OFF times, and discharge current levels. They determined the optimum operating conditions for higher circularity that improved the overall drilled hole accuracy value. Tapering of holes is another important element of EDM drilling in an aluminium-based MMC. Thakur et al. (2022) observed that the change in hole taper with pulsing duration, interspacing time between pulses, and discharge current in Al/Mg MMCs. Researchers discovered that it was possible to minimize the taper in holes and increase the dimensional accuracy for drilled holes using the best set of process parameters. The settings for the Electric Discharge Machining (EDM) Drill Process significantly affect the machinability of MMCs' high-strength aluminium-based metal matrix composites. A detailed consideration was done by Reddy et al. (2021) for Al/SiC MMCs under the response surface methodological approach where discharge current, distilled water pressure, pulse on-time as well, and pulse off-time were optimized. In order to define the correct operating conditions for an effective EDM drill, their research focused on factors related to hole taper, surface roughness, and material erosion percentage. Similarly, Sandhu et al. (2022) compared different Al/Al₂O₃ MMCs to determine the effect on drilled holes as well as HAZ and MRMD. These comparisons provided valuable information on how process parameters affect the drillability of Al₂O₃-based aluminium-reinforced MMC.

The effect of discharge current on the efficiency of EDM drilling in aluminium MMCs was also investigated. Kumar et al. (2021) investigated the relationship between surface treatment and the diameter of Al/SiC MMCs at discharge current. This study aimed to investigate the circularity of exit and entrance passages. This allowed them to determine the accuracy of the sizes of these passages at different liquid discharges. Mallick et al. (2022) also improved the EDM parameters to produce circular holes in Al/CNT laminates. Appropriate choices of discharge current, pulse on time, and pulse off time resulted in improved hole roundness values, improving hole quality in the aluminium-based MMC.

To this end, the researchers investigated various aspects affecting the dimensions of holes drilled by EDM, including surface quality and integrity. By controlling surface roughness and hole bevel through pulse on time, pulse off time, discharge current and distilled water pressure settings, dimensional accuracy and mechanical

properties can be maintained in drilled holes. These collaborative investigations improve our understanding of the relationship between EDM drilling parameters and high-performance aluminium-based metal matrix composites and provide valuable information for process improvement related to various engineering fields.

Process variables such as surface integrity and quality in EDM drilling for aluminium-based MMC are significant, and researchers have attempted to establish links between these entities. On the other hand, Gudipudi et al. (2022) investigated the effect of distilled water pressure and pulsing time on hole narrowing and surface roughness in Al/Mg MMC. In other words, by evaluating the effect of changing specific parameters in this EDM drilling process, the researchers uncovered valuable insights into the consistency of the size and smoothness of the holes produced, which helped to increase the overall efficiency of this machining process for these composites.

Another thing researched is the application of the latest drilling optimisation approaches in order to raise the performance level of EDM drilling. Kumar et al. (2022), used an approach to multi-objective optimization in a study so as to determine the optimal set of process parameters for Al/SiC MMCs. For this reason, the process considered such as surface roughness, material removal rate, and wear on electrode were all combined as parallel aims for effective evaluation of EDM drilling performance. This paper showed how MOO can be used to enhance the efficiency of drilling operations in a magnesium-based alloy MMC. Muni et al. (2022) studied how micro-structural characteristics influence the EDM performance, such as particle shapes and distributions in Al/Al₂O₃ MMC's. The result indicated that microstructure greatly influenced the rate of material removal and the outcome of holes, hence the need to understand composite microstructure in order to improve the EDM drilling process.

Key Findings from the literature

1. Influence of Reinforcing Material:

The choice of reinforcing material has a profound influence on the mechanical properties of Al-based MMCs. It was found that using metallic reinforcements (such as Al, Mg) and ceramic particles like SiC and Al₂O₃ enhances the composites' tensile strength, hardness, and resistivity to wear.

2. Fabrication Techniques:

Several methods for fabricating Alum MMCs have been developed such as in situ synthesis, powder metallurgy and stir cast. Each method has its own advantages in regard to ensuring homogenous distribution

of strengthening agents and regulating the microstructure at the same time.

3. Process Parameter Optimization:

The drilling performance in aluminium-based metal matrix composites is significantly affected by the EDM drilling parameters, which include discharge current, distilled water pressure, pulse on time, and pulse off time. Therefore, it is crucial to ensure that the above- stated elements are appropriately considered for optimal material removal as well as improved surface quality.

4. Advanced Optimization approaches:

Various advanced optimization techniques such as Response Surface Methodology (RSM) and multi-objective optimization have been applied to this end to improve the results in EDM drilling. Such approaches are complex. They consider a number of quality factors simultaneously; giving comprehensive evaluation; providing high effectiveness to the processes.

Proposed Methodology

The proposed method, which entails four steps, can be observed in Figure one. At the first stage of composite production, the required Aluminium-Based Metal Matrix Composite is fabricated making use of suitable reinforcements and fabrication procedures. In the second step, the produced composite undergoes rigorous testing to evaluate its mechanical properties and determine if it can be used for a specific purpose. Thirdly, we now look closely at how the drilling process occurs. The composite is made through EDM drilling with stringent process parameter controls such as pulse on time, pulse off-time, distilled water pressure, and discharge current. This particular step aims to drill as effectively and accurately as possible without damaging the composite material.

The final step involves modelling and optimisation. The previous phase's data is assessed, and mathematical models that relate the input parameters with drilling performance indicators are established. After this, using these models for optimizing allows one to identify an operating envelope from the input parameters in which perfect drilling takes place at minimal risk. These four phases of methodology will be applied in this research aimed at studying a whole manufacturing process from cutting composites to EDM cutting. Furthermore, this study aims at providing useful data that will come in handy during subsequent improvements and applications of aluminium-magnesium metal matrix composites and their machinability approaches.

Fabrication of composite

Researchers are working to create novel and cutting-edge composite materials in response to the growing need for lightweight, highly durable materials. One of the most widely utilized basic materials for the creation of these metal matrix alloys is aluminium. A great deal of research has gone into creating and developing aluminium alloys. AA2024, one of the most widely used Al alloys, is widely utilized in the aerospace sector. Nonetheless, a sensible proportionate addition of SiC and Mg can enhance the AA 2024's characteristics.

Adding silicon carbide (SiC) and magnesium (Mg) to the alloy results in an aluminium-based metal matrix composite (MMC) with better mechanical properties than the original AA2024 alloy. The addition of SiC and Mg as reinforcing elements can lead to a number of improvements:

1. Increased strength:

SiC is a strong and hard material, and its addition to the aluminium matrix as a reinforcing phase can significantly increase the composite's hardness, yield strength and tensile strength. The reinforcing action of SiC enhances the overall structural integrity and load-bearing capacity of the composite.

2. Increased Stiffness:

The incorporation of SiC also increases the stiffness and modulus of the composite, making it less prone to deformation when stress is applied.

3. Higher wear resistance:

SiC particles are suitable for applications involving sliding contact and abrasive wear because they have excellent wear resistance, which also applies to MMC.

4. Reduced coefficient of thermal expansion (CTE):

The composite expands less thermally because SiC has a lower coefficient of thermal expansion than aluminium. This function is useful in situations where it is important to maintain dimensions during temperature changes.

5. Lightweight:

The low densities of SiC and Mg help the composite remain lightweight while preserving the beneficial properties of aluminium alloys.

6. Enhanced Damping Capacity:

The composite may be better suited for vibration-damping applications if magnesium is present in it. Therefore, the current study introduces SiC and Mg to the AA2024 alloy.

The procedure of fabricating the composite stir-casting has been implemented. The AA2024 alloy has

been combined with SiC and magnesium powder. The Table contains a list of the weight percentage of the materials taken.

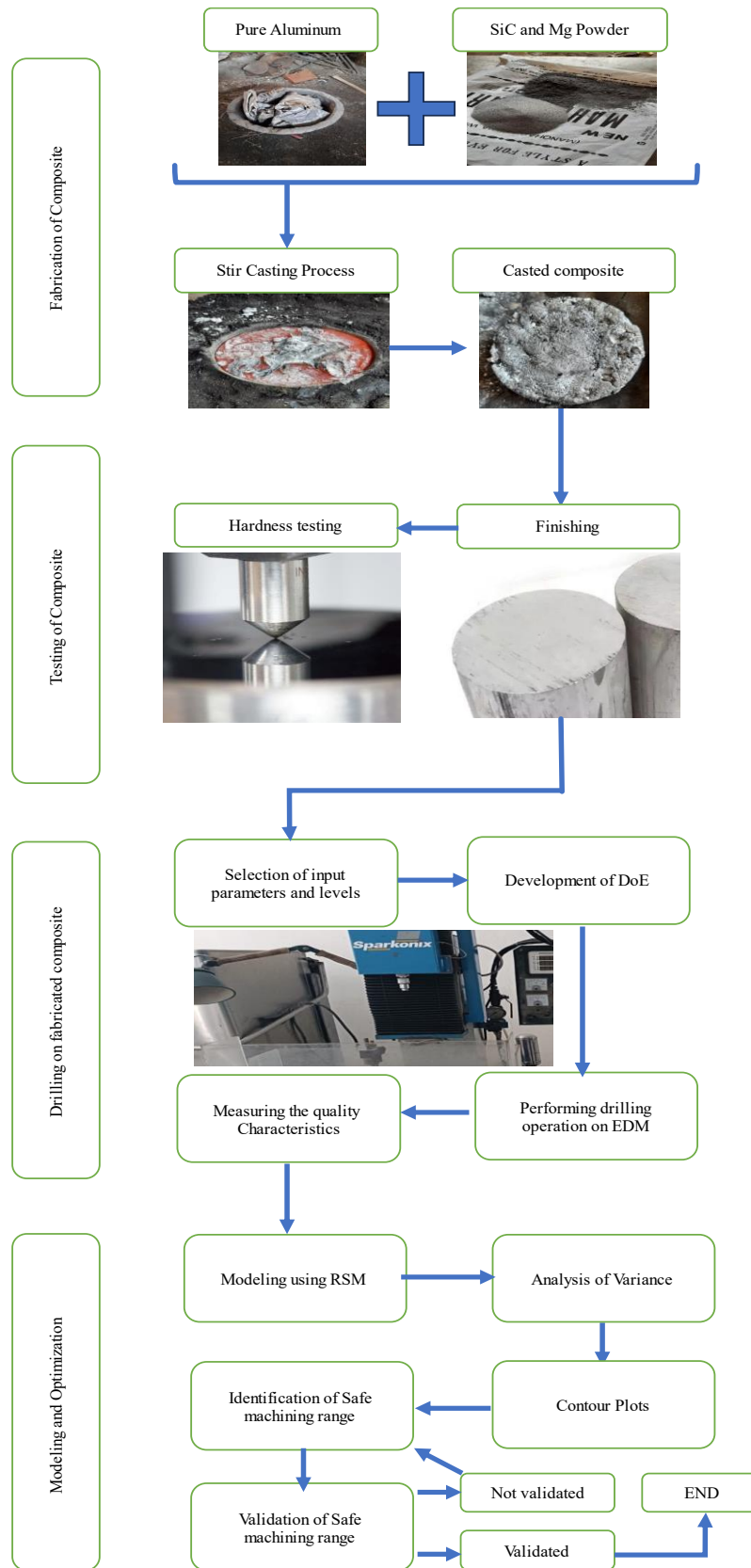


Figure 1. Flow chart of the proposed methodology.

Table 1. Composition of the composite.

| AA2024 | Mg | SiC |
|-------------|------|-----|
| Remaining % | 1.5% | 10% |

SiC's volume percentage in MMCs can often vary from 5% to 30%. Greater volume fractions of SiC will have a more substantial effect, but they may also make it more difficult to distribute the reinforcing particles evenly throughout the aluminium matrix as it is being fabricated.

Usually, magnesium is added as an alloying element in the aluminium matrix instead of as a distinct phase like SiC particles. Usually, AA2024 alloy has a magnesium percentage of 1.2% to 1.8%. In Figure 2, the stir-casting setup is displayed.

The Rockwell hardness testing apparatus was used to measure the composite's hardness after it was fabricated. A major load of 100 kg and a minor load of 10 kg each have been applied to three samples. Table 2 contains a listing of the acquired hardness number. To reduce inaccuracies, an average of the obtained hardness has been taken.

Table 2 shows that the manufactured composite has a hardness of 68, which is significantly higher than the AA2024. The exact temper and heat treatment of the AA2024 alloy can affect its Rockwell hardness. As

**Figure 2. Stir casting setup.**

previously stated, the approximate ranges for the Rockwell hardness values of AA2024 for various tempers are as follows:

AA2024-T3: Rockwell hardness (HRC) range is around 35 to 45.

AA2024-T4: The Rockwell hardness (HRC) ranges from 40 to 50.

AA2024-T6: Rockwell hardness (HRC) is around 50-60.

AA2024-T8: The Rockwell hardness (HRC) ranges from 40 to 50.

certain conditions; SiC particles can be abrasive and may cause increased tool wear during machining, necessitating appropriate tooling and machining parameters. Considering the issue, it is unsuitable to machine the composite using a conventional machining process. Hence, the electric discharge machine has been used for the drilling operation.

The input parameters and levels selected for the machining have been listed in Table 3. The fabricated composite has been taken as a sheet of 2 mm thickness.

Table 2. Hardness Testing

| Trial No. | Specimen | Indenter Type | Load Applied | Rockwell Scale | Rockwell hardness number |
|-----------|------------------------|---------------|-------------------------------------|----------------|--------------------------|
| 1 | AA2024+1.5% Mg+10% SiC | Ball Indenter | Minor Load=10kg Major Load=100kg | B | 70 |
| 2 | AA2024+1.5% Mg+10% SiC | Ball Indenter | Minor Load=10kg Major Load=100kg | B | 66 |
| 3 | AA2024+1.5% Mg+10% SiC | Ball Indenter | Minor Load=10kg Major Load=100kg | B | 68 |
| Average | | | | | 68 |

Table 3. Selected parameters and levels.

| Input Parameters | Level 1 | Level 2 | Level 3 |
|--|---------|---------|---------|
| Pulse on time (μ s) | 8 | 9 | 10 |
| Distilled water pressure (kg/cm^2) | 60 | 70 | 80 |
| Discharge current (A) | 14 | 15 | 16 |

Table 4. Other parameters that have been kept constant.

| Parameter | Constant value |
|--------------------|-----------------|
| Pulse off-time | 10 (μ s) |
| Electrode Material | Copper |
| Dielectric fluid | Deionized water |
| Tool Diameter | 0.5 mm |
| Flushing Method | Side flushing |

Machining of the Composite

The machining of AA2024 experiences several challenges during machining. With the addition of SiC and Mg to AA2024, the issue may increase as the addition of SiC and Mg increases the composite's strength, which may lead to a reduction in ductility compared to the base Aluminium alloy. This could impact the composite's ability to deform plastically under

The other parameters that were kept constant throughout the experimentation are listed in Table 4.

After finalizing the parameters and levels, the design of the experiment (DoE) has been developed based on the Box-Behnken design (BBD) (Ferreira et al., 2007). Table 5 shows the BBD-based DoE.

After finalizing the DoE experiments that have been performed on the EDM machine, the actual image of the machine has been shown in Figure 3.

Table 5. BBD based DoE.

| Experiment No. | Pulse on time (μs) P_{on} | Distilled water pressure (kg/cm^2) D_w | Discharge current (A) D_c |
|----------------|--|---|--------------------------------|
| 1 | 8 | 70 | 16 |
| 2 | 10 | 70 | 16 |
| 3 | 9 | 80 | 14 |
| 4 | 9 | 70 | 15 |
| 5 | 10 | 80 | 15 |
| 6 | 10 | 70 | 14 |
| 7 | 8 | 60 | 15 |
| 8 | 9 | 70 | 15 |
| 9 | 8 | 80 | 15 |
| 10 | 8 | 70 | 14 |
| 11 | 10 | 60 | 15 |
| 12 | 9 | 80 | 16 |
| 13 | 9 | 60 | 16 |
| 14 | 9 | 60 | 14 |
| 15 | 9 | 70 | 15 |



Figure 3. EDM machine



Figure 4. Traveling Microscope

During the experimentation, each experiment has been performed thrice and the obtained drills have been examined using a traveling microscope as shown in Figure 4. With the help of this microscope, the diameters at the entry and exit of the drilled holes have been measured and an average of the same has been taken to measure the mean diameter of the drill.

Moreover, from the obtained values of the diameters at entry and exit, hole circularity at the entry, hole circularity at the exit, and hole taper have also been measured using the equations;

$$\text{Hole circularity at entry } (C_{\text{entry}}) = \frac{(d_{\text{min.}})_{\text{entry}}}{(d_{\text{max.}})_{\text{entry}}} \quad (1)$$

$$\text{Hole circularity at exit } C_{\text{exit}} = \frac{(d_{\text{min.}})_{\text{exit}}}{(d_{\text{max.}})_{\text{exit}}} \quad (2)$$

$$\text{Hole Taper} = \tan^{-1} (C_{\text{entry}} - C_{\text{exit}}) / 2h \quad (3)$$

Where d_{min} is the measured minimum entry diameter of a drill, d_{max} is the measured maximum diameter of a drill, and h is the thickness of the workpiece. Table 6 shows the measured values of all the responses.

Results and Discussion

The obtained responses have circularity at entry, exit, and hole taper values. All three parameters are preferred to be minimum. However, in the case of hole, circularity should be closer to 1 for optimum solution. The hole taper is a dependable output but the value of the hole taper is considerable because by optimizing it the deviation in the entry and exit side of the circularity can be optimized.

In the present work, the obtained responses at the given set of input parameters have been used to generate

mathematical models using response surface methodology (Shrivastava and Singh, 2021; Jain et al., 2020). The generated models have been listed in equations 4-6. Moreover, the associated R-sq value of the models has been listed in Table 7. From the R-sq values, it is clear that the models are significant (Myers et al., 2009).

Moreover, to identify the accuracy of the model's deviation between the experimental and predicted values has been calculated. The percentage deviations that were obtained are listed in Table 8.

The comparison in Table 8 shows that the average percentage deviation in the experimental and predicted values of hole circularity at entry, exit, and hole taper is

Table 6. Measured values of responses.

| Experiment No. | P _{on} | D _w | D _c | C _{entry} | C _{exit} | Hole Taper |
|----------------|-----------------|----------------|----------------|--------------------|-------------------|------------|
| 1 | 8 | 70 | 16 | 0.724 | 0.589 | 0.034 |
| 2 | 10 | 70 | 16 | 0.843 | 0.639 | 0.050 |
| 3 | 9 | 80 | 14 | 0.706 | 0.568 | 0.034 |
| 4 | 9 | 70 | 15 | 0.733 | 0.600 | 0.033 |
| 5 | 10 | 80 | 15 | 0.787 | 0.545 | 0.059 |
| 6 | 10 | 70 | 14 | 0.788 | 0.605 | 0.045 |
| 7 | 8 | 60 | 15 | 0.668 | 0.524 | 0.036 |
| 8 | 9 | 70 | 15 | 0.733 | 0.600 | 0.033 |
| 9 | 8 | 80 | 15 | 0.838 | 0.510 | 0.079 |
| 10 | 8 | 70 | 14 | 0.745 | 0.612 | 0.033 |
| 11 | 10 | 60 | 15 | 0.851 | 0.612 | 0.059 |
| 12 | 9 | 80 | 16 | 0.892 | 0.607 | 0.069 |
| 13 | 9 | 60 | 16 | 0.735 | 0.574 | 0.040 |
| 14 | 9 | 60 | 14 | 0.756 | 0.612 | 0.036 |
| 15 | 9 | 70 | 15 | 0.733 | 0.600 | 0.033 |

$$\begin{aligned}
 C_{Entry} = & 10.97 - 0.346 P_{on} - 0.0581 D_w - 0.946 D_c \\
 & + 0.0280 P_{on} * P_{on} + 0.000255 D_w * D_w \\
 & + 0.0146 D_c * D_c - 0.00583 P_{on} * D_w + 0.0192 \\
 & P_{on} * D_c + 0.00517 D_w * D_c
 \end{aligned}
 \tag{4}$$

$$\begin{aligned}
 C_{Exit} = & 6.55 + 0.183 P_{on} + 0.0332 D_w - 1.066 D_c - \\
 & 0.01565 P_{on} * P_{on} - 0.000365 D_w * D_w \\
 & + 0.02685 D_c * D_c - 0.001330 P_{on} * D_w + \\
 & 0.01420 P_{on} * D_c + 0.001920 D_w * D_c
 \end{aligned}
 \tag{5}$$

$$\begin{aligned}
 \text{Hole Taper} = & 1.09 - 0.1281 P_{on} - 0.02187 D_w + 0.026 D_c \\
 & + 0.01047 P_{on} * P_{on} + 0.000148 D_w * D_w \\
 & - 0.00285 D_c * D_c - 0.001063 P_{on} * D_w + \\
 & 0.00120 P_{on} * D_c + 0.000774 D_w * D_c
 \end{aligned}
 \tag{6}$$

4.547%, 2.123%, and 7.20%, respectively. Hence, the models are at least 92.8% accurate. Furthermore, to identify the significant parameter, an ANOVA analysis was done. Table 9-11 shows the ANOVA (Arora et al., 2023; Jain et al., 2019; Arora et al., 2023) analysis for hole circularity at entry, exit, and hole taper, respectively.

Table 7. R-sq values of the models

| Model | R-sq value |
|--------------------|------------|
| C _{entry} | 95.94% |
| C _{exit} | 92.07% |
| Hole taper | 91.96% |

Table 8. Comparison between experimental and predicted values

| Experiment No. | Exp value of Centry | Pred value of Centry | Percentage Deviation in Centry | Exp value of Cexit | Pred value of Cexit | Percentage deviation in Cexit | Exp value of hole taper | Pred value of hole taper | Percentage Deviation in hole taper |
|----------------|---------------------|----------------------|--------------------------------|--------------------|---------------------|-------------------------------|-------------------------|--------------------------|------------------------------------|
| 1 | 0.724 | 0.782 | 7.981 | 0.589 | 0.589 | 0.051 | 0.034 | 0.041 | 21.12 |
| 2 | 0.843 | 0.896 | 6.285 | 0.639 | 0.659 | 3.208 | 0.050 | 0.051 | 2.96 |
| 3 | 0.706 | 0.753 | 6.697 | 0.568 | 0.570 | 0.343 | 0.034 | 0.041 | 20.26 |
| 4 | 0.733 | 0.767 | 4.652 | 0.600 | 0.611 | 1.867 | 0.033 | 0.033 | 0.70 |
| 5 | 0.787 | 0.827 | 5.083 | 0.545 | 0.556 | 2.064 | 0.059 | 0.061 | 2.97 |
| 6 | 0.788 | 0.799 | 1.444 | 0.605 | 0.628 | 3.752 | 0.045 | 0.038 | 15.29 |
| 7 | 0.668 | 0.698 | 4.431 | 0.524 | 0.535 | 2.147 | 0.036 | 0.035 | 2.81 |
| 8 | 0.733 | 0.767 | 4.652 | 0.600 | 0.611 | 1.867 | 0.033 | 0.033 | 0.70 |
| 9 | 0.838 | 0.868 | 3.556 | 0.510 | 0.540 | 5.971 | 0.079 | 0.074 | 6.19 |
| 10 | 0.745 | 0.762 | 2.279 | 0.612 | 0.614 | 0.278 | 0.033 | 0.033 | 1.15 |

| | | | | | | | | | |
|------------------------------|-------|-------|--------|------------------------------|-------|--------|------------------------------|-------|-------|
| 11 | 0.851 | 0.890 | 4.583 | 0.612 | 0.604 | 1.266 | 0.059 | 0.064 | 8.73 |
| 12 | 0.892 | 0.915 | 2.565 | 0.607 | 0.612 | 0.783 | 0.069 | 0.067 | 2.42 |
| 13 | 0.735 | 0.758 | 3.113 | 0.574 | 0.595 | 3.615 | 0.040 | 0.034 | 15.02 |
| 14 | 0.756 | 0.803 | 6.228 | 0.612 | 0.630 | 2.900 | 0.036 | 0.039 | 6.97 |
| 15 | 0.733 | 0.767 | 4.652 | 0.600 | 0.611 | 1.867 | 0.033 | 0.033 | 0.70 |
| Average Percentage Deviation | | | 4.547% | Average Percentage Deviation | | 2.132% | Average Percentage Deviation | | 7.20% |

Table 9. ANOVA analysis for hole circularity at entry

| Source | DF | Adj SS | Adj MS | F-Value | P-Value |
|--------------------------|----|----------|----------|---------|---------|
| Model | 9 | 0.052538 | 0.005838 | 13.12 | 0.006 |
| Linear | 3 | 0.021445 | 0.007148 | 16.06 | 0.005 |
| Pon | 1 | 0.010804 | 0.010804 | 24.28 | 0.004 |
| Dw | 1 | 0.005660 | 0.005660 | 12.72 | 0.016 |
| Dc | 1 | 0.004980 | 0.004980 | 11.19 | 0.020 |
| Square | 3 | 0.005331 | 0.001777 | 3.99 | 0.085 |
| Pon*Pon | 1 | 0.002884 | 0.002884 | 6.48 | 0.052 |
| Dw*Dw | 1 | 0.002392 | 0.002392 | 5.37 | 0.068 |
| Dc*Dc | 1 | 0.000782 | 0.000782 | 1.76 | 0.242 |
| 2-Way Interaction | 3 | 0.025762 | 0.008587 | 19.30 | 0.004 |
| Pon*Dw | 1 | 0.013596 | 0.013596 | 30.55 | 0.003 |
| Pon*Dc | 1 | 0.001475 | 0.001475 | 3.31 | 0.128 |
| Dw*Dc | 1 | 0.010692 | 0.010692 | 24.03 | 0.004 |
| Error | 5 | 0.002225 | 0.000445 | | |
| Lack-of-Fit | 3 | 0.002225 | 0.000742 | * | * |
| Pure Error | 2 | 0.000000 | 0.000000 | | |
| Total | 14 | 0.054763 | | | |

Table 10. ANOVA analysis for hole circularity at the exit

| Source | DF | Adj SS | Adj MS | F-Value | P-Value |
|---------------|----|----------|----------|---------|---------|
| Model | 9 | 0.016555 | 0.001839 | 6.45 | 0.027 |
| Linear | 3 | 0.004531 | 0.001510 | 5.30 | 0.052 |
| Pon | 1 | 0.003428 | 0.003428 | 12.03 | 0.018 |

| | | | | | |
|--------------------------|----|----------|----------|-------|-------|
| Dw | 1 | 0.001086 | 0.001086 | 3.81 | 0.108 |
| Dc | 1 | 0.000017 | 0.000017 | 0.06 | 0.818 |
| Square | 3 | 0.009036 | 0.003012 | 10.57 | 0.013 |
| Pon*Pon | 1 | 0.000904 | 0.000904 | 3.17 | 0.135 |
| Dw*Dw | 1 | 0.004933 | 0.004933 | 17.31 | 0.009 |
| Dc*Dc | 1 | 0.002662 | 0.002662 | 9.34 | 0.028 |
| 2-Way Interaction | 3 | 0.002989 | 0.000996 | 3.50 | 0.106 |
| Pon*Dw | 1 | 0.000708 | 0.000708 | 2.48 | 0.176 |
| Pon*Dc | 1 | 0.000807 | 0.000807 | 2.83 | 0.153 |
| Dw*Dc | 1 | 0.001475 | 0.001475 | 5.17 | 0.072 |
| Error | 5 | 0.001425 | 0.000285 | | |
| Lack-of-Fit | 3 | 0.001425 | 0.000475 | * | * |
| Pure Error | 2 | 0.000000 | 0.000000 | | |
| Total | 14 | 0.017980 | | | |

Table 11. ANOVA analysis for hole taper

| Source | DF | Adj SS | Adj MS | F-Value | P-Value |
|--------------------------|----|----------|----------|---------|---------|
| Model | 9 | 0.002951 | 0.000328 | 6.36 | 0.028 |
| Linear | 3 | 0.001039 | 0.000346 | 6.71 | 0.033 |
| Pon | 1 | 0.000129 | 0.000129 | 2.49 | 0.175 |
| Dw | 1 | 0.000656 | 0.000656 | 12.73 | 0.016 |
| Dc | 1 | 0.000254 | 0.000254 | 4.92 | 0.077 |
| Square | 3 | 0.001214 | 0.000405 | 7.85 | 0.024 |
| Pon*Pon | 1 | 0.000405 | 0.000405 | 7.85 | 0.038 |
| Dw*Dw | 1 | 0.000810 | 0.000810 | 15.70 | 0.011 |
| Dc*Dc | 1 | 0.000030 | 0.000030 | 0.58 | 0.480 |
| 2-Way Interaction | 3 | 0.000698 | 0.000233 | 4.51 | 0.069 |
| Pon*Dw | 1 | 0.000452 | 0.000452 | 8.77 | 0.031 |
| Pon*Dc | 1 | 0.000006 | 0.000006 | 0.11 | 0.751 |
| Dw*Dc | 1 | 0.000240 | 0.000240 | 4.65 | 0.084 |
| Error | 5 | 0.000258 | 0.000052 | | |
| Lack-of-Fit | 3 | 0.000258 | 0.000086 | * | * |
| Pure Error | 2 | 0.000000 | 0.000000 | | |
| Total | 14 | 0.003209 | | | |

From the ANOVA analysis, it has been found that the hole circularity at entry and exit, Pon, is the most significant parameter. Similarly, Dw is the most significant parameter for hole taper, as the P-values of these parameters are less than 0.05. Now, considering the need to optimize the models, much work has already been reported in this domain. However, it is very clear from the reported works that, whenever a generated model is optimized, either local optimization is considered or global. Local optimization only gives results for the selected input combination, considering multiple objectives at a time. However, global optimization optimizes the responses for the entire range of input parameters. In the process, it has been reported by the

researchers that the obtained optimal set is most of the time not feasible for the machine. Hence, taking the round of the parameter is usually considered. However, the obtained result due to this rough-off deviates a lot from the expected result. To resolve this existing issue, the authors have adopted a new methodology for obtaining a suitable range of input parameters about minimum values of responses (Shrivastava and Singh, 2021). Following the methodology, the authors have developed contour plots using the mathematical equations 4-6. The generated contour plots have been shown in Figures 5-13. Figures 5-7 show the variation in hole circularity with the change in input parameters. Here, the target is to maximize the hole circularity as close as

possible to 1. The red color in the 3D contour plot shows the minimum value of hole circularity, the yellow color indicates the moderate value and the blue/ violet color indicates the maximum value of hole circularity. In the

be treated as trending to 1 or maximum value. Accordingly, the range of input parameters about hole circularity at entry greater than 0.75 has been ascertained from the contour plots 5-7, as listed in Table 12. In Table

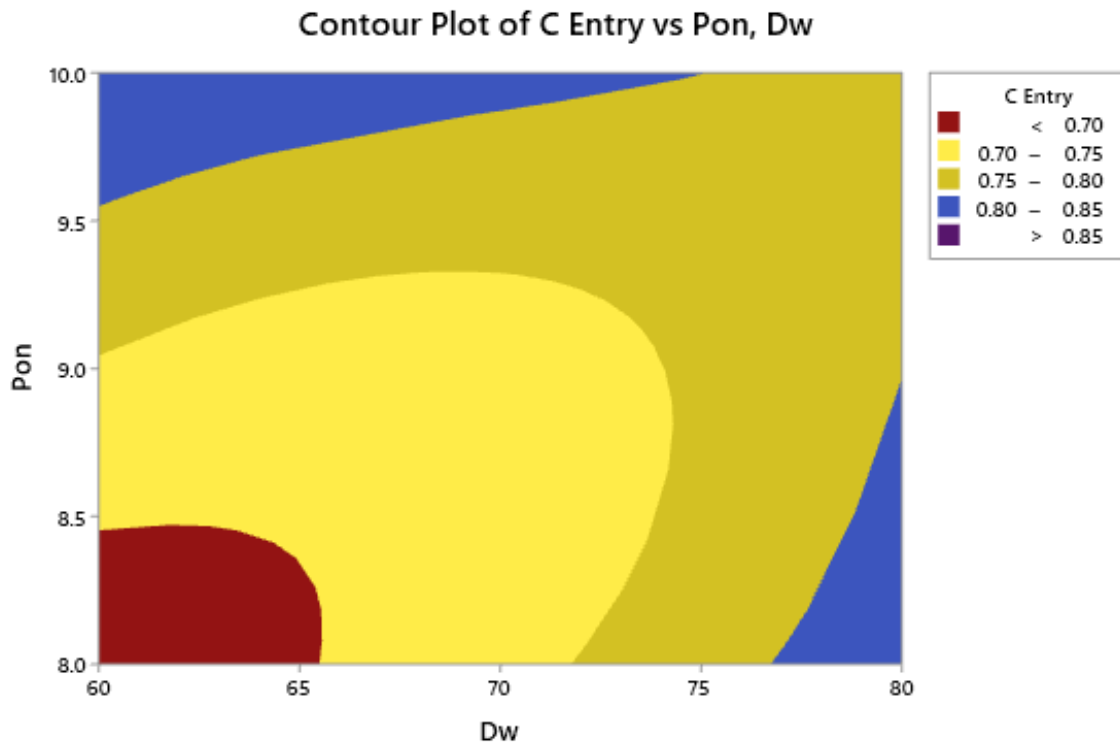


Figure 5. Contour plot of hole circularity at entry versus pulse on time and distilled water pressure

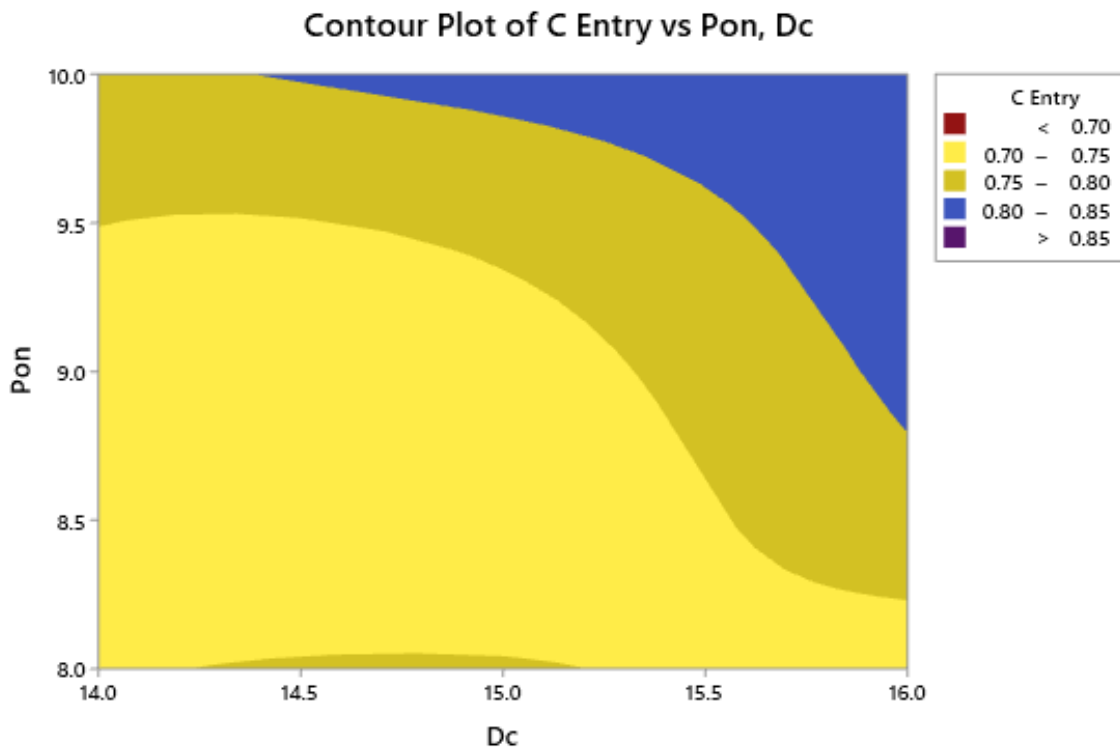


Figure 6. Contour plot of hole circularity at entry versus pulse on time and discharge current

present work, it has been considered for analysis that the value of hole circularity at entry, if greater than 0.75, can

12, an intersection range for hole circularity at entry was also evaluated by taking the intersection of obtained

values from different plots. This intersection range pertains to hole circularity at entry greater than 0.75.

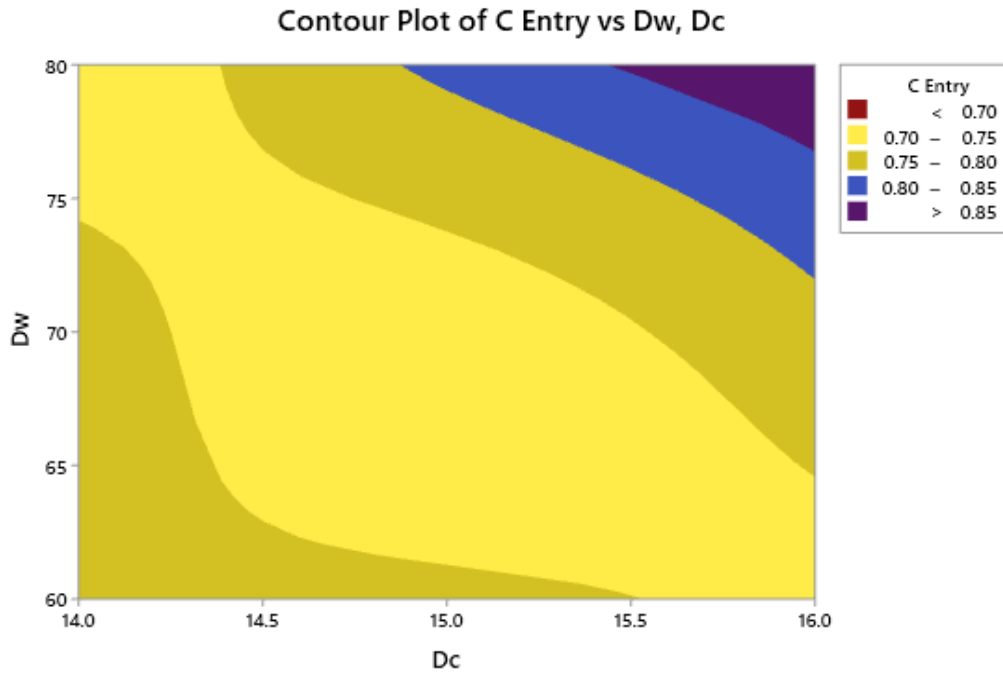


Figure 7. Contour plot of hole circularity at entry versus distilled water pressure and discharge current

Table 12. A suitable range for maximum hole circularity at entry

| Parameter | C Entry vs Pon, Dw | C Entry vs Pon, Dc | C Entry vs Dw, Dc | Intersection range |
|-----------|--------------------|--------------------|-------------------|--------------------|
| Pon | 9.2-10 | 9.5-10 | | 9.5-10 |
| Dw | 73-80 | | 73-80 | 73-80 |
| Dc | | 14-16 | 15.3-16 | 15.3-16 |

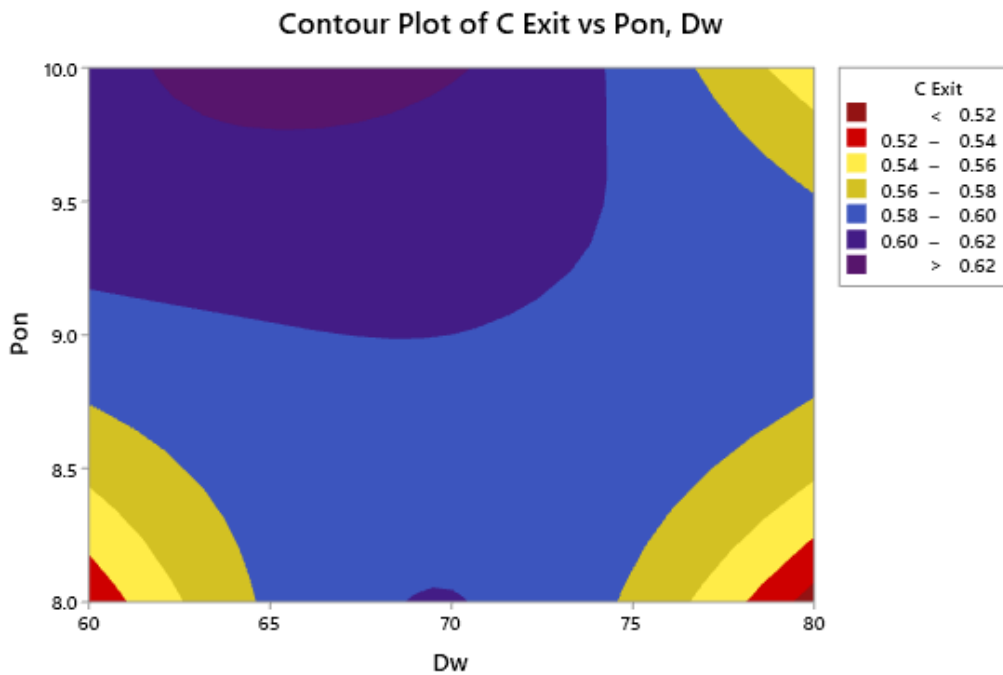


Figure 8. Contour plot of hole circularity at exit versus pulse on time and distilled water pressure

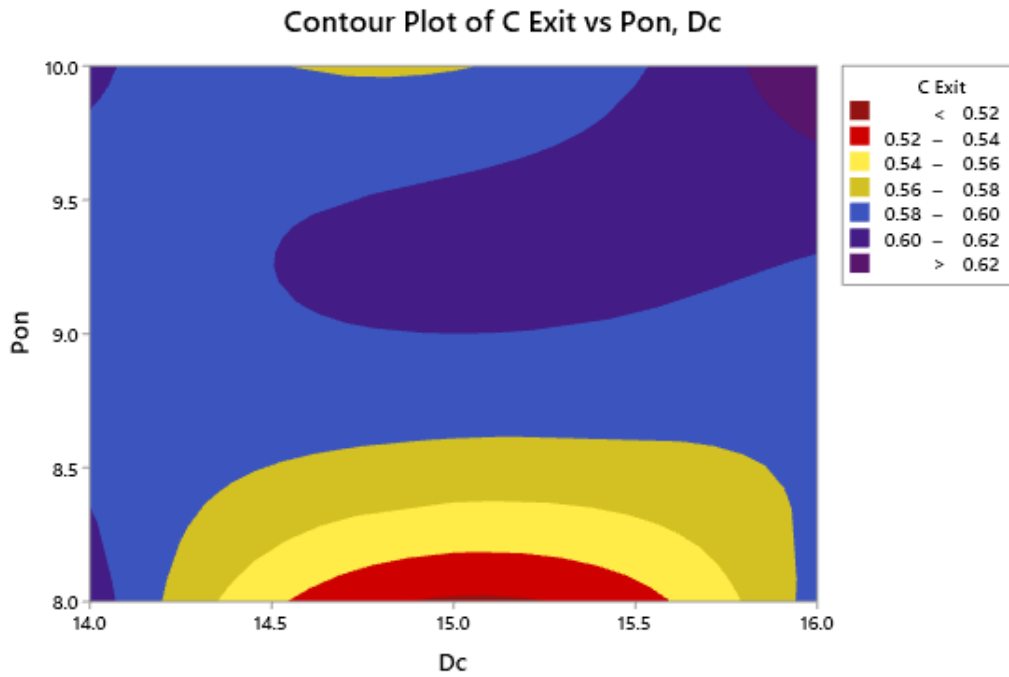


Figure 9. Contour plot of hole circularity at exit versus pulse on time and discharge current

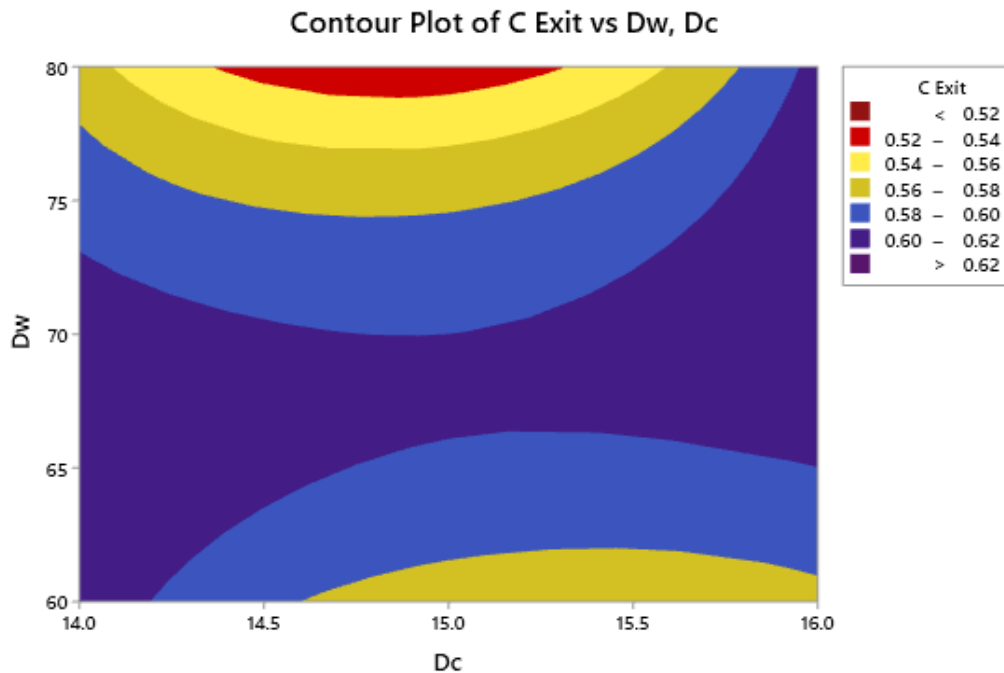


Figure 10. Contour plot of hole circularity at exit versus distilled water pressure and discharge current

Table 13. A suitable range for maximum hole circularity at the exit

| Parameter | C Exit vs Pon, Dw | C Exit vs Pon, Dc | C Exit vs Dw, Dc | Intersection range |
|-----------|-------------------|-------------------|------------------|--------------------|
| Pon | 8.7-10 | 8.6-9.9 | | 8.7-9.9 |
| Dw | 60-77 | | 62-76 | 62-76 |
| Dc | | 14-16 | 14-16 | 14-16 |

Similarly, Figure 8-10 shows the variation in hole circularity at exit with the change in input parameters. Here, the target is to maximize the hole circularity, as close as possible to 1. The red color in the 3D contour

plot shows the minimum value of hole circularity, the yellow color indicates the moderate value and the blue/violet color indicates the maximum value of hole circularity. In the present work, it has been considered for

analysis that the value of hole circularity at exit, if greater than 0.58, can be treated as trending to 1 or maximum value. Accordingly, the range of input parameters

Table 13. In Table 12 an intersection range for hole circularity at exit has also been evaluated by taking the intersection of obtained values from different plots. This

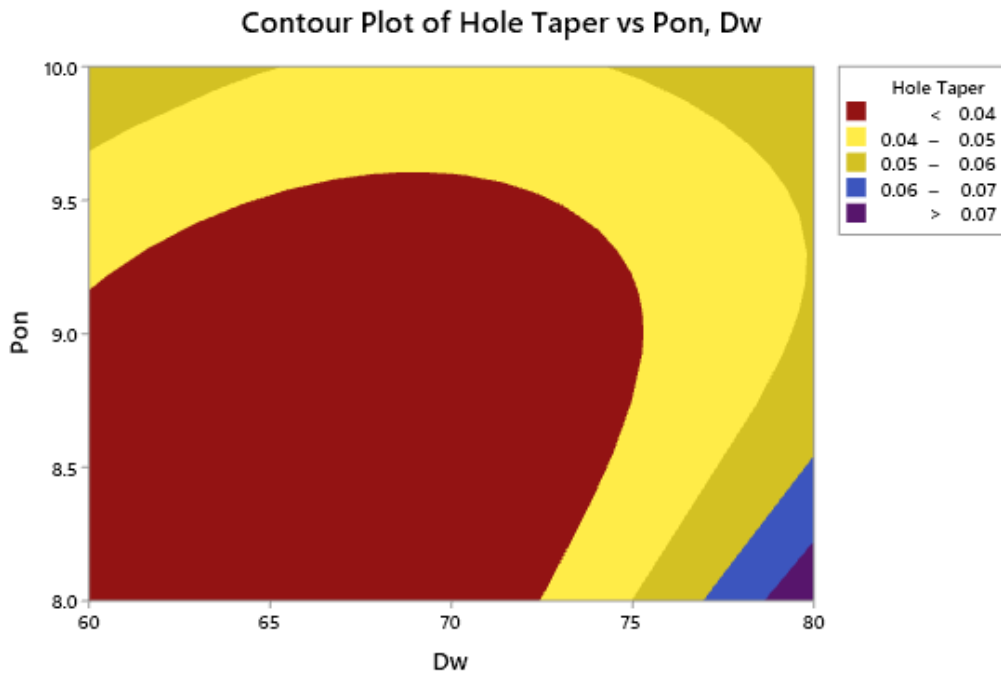


Figure 11. Contour plot of hole taper versus pulse on time and distilled water pressure

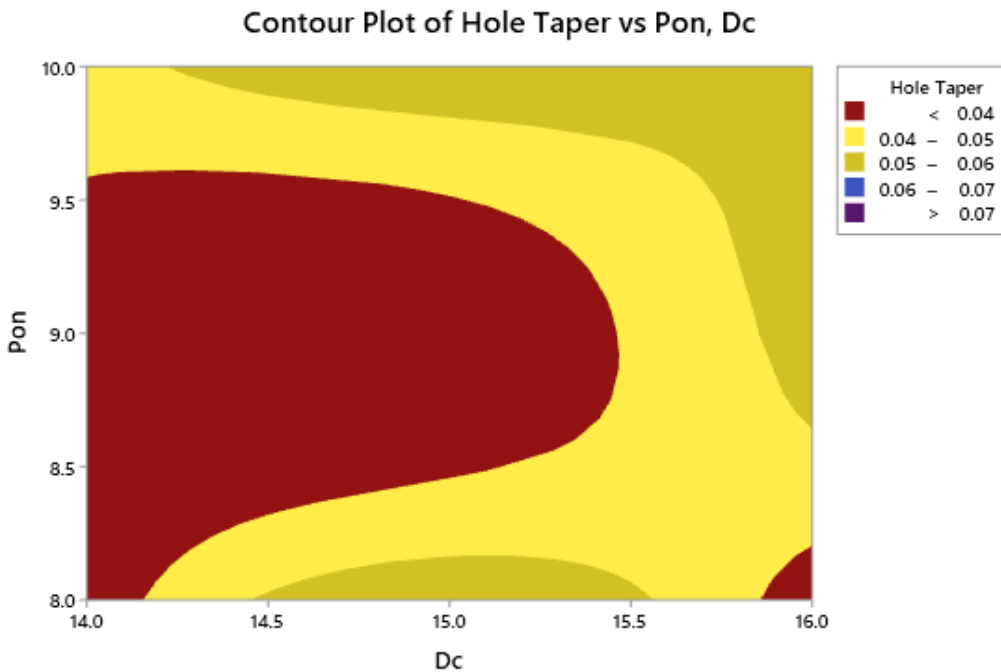


Figure 12. Contour plot of hole taper versus pulse on time and discharge current

Table 14. A suitable range for minimum hole taper

| Parameter | Hole taper vs Pon, Dw | Hole taper vs Pon, Dc | Hole taper vs Dw, Dc | Intersection range |
|-----------|-----------------------|-----------------------|----------------------|--------------------|
| Pon | 8-9.7 | 8.2-9.7 | | 8.2-9.7 |
| Dw | 60-75 | | 60-76 | 60-75 |
| Dc | | 14-15.6 | 14-15.6 | 14-15.6 |

pertaining to hole circularity at exit greater than 0.75 has been ascertained from the contour plots 8-10, as listed in

intersection range pertains to hole circularity at exit greater than 0.58.

Similarly, Figure 11-13 shows the variation in hole taper with the change in input parameters. Here, the target is to minimize the hole taper, as close as possible to 0. The red color in the 3D contour plot shows the minimum value of hole circularity, yellow indicates the moderate value, and blue/violet indicates the maximum value of hole taper. In

parameters was identified by taking the intersection of the ranges obtained in Tables 12-14. The intersection range for precise drilling has been listed in Table 15.

To validate the obtained range of input parameters as listed in Table 15. Validation experiments have been performed, and the quality characteristics have been

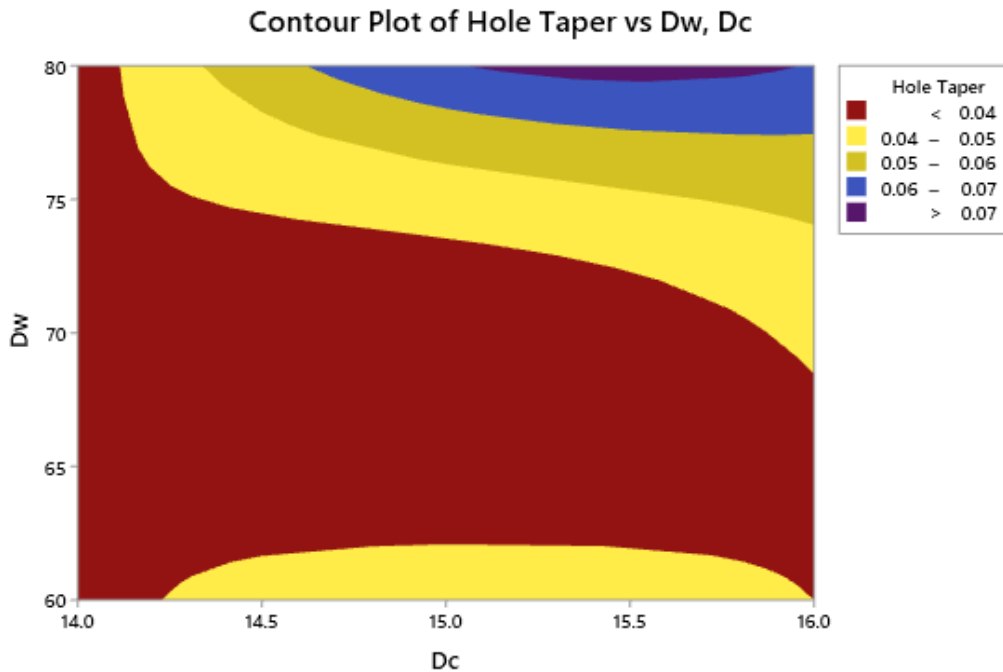


Figure 13. Contour plot of hole taper versus distilled water pressure and discharge current

Table 15. Intersection range for precise drilling

| Parameter | Hole circularity at entry | Hole circularity at the exit | Hole taper | Intersection range |
|-----------|---------------------------|------------------------------|------------|--------------------|
| Pon | 9.5-10 | 8.7-9.9 | 8.2-9.7 | 9.5-9.7 |
| Dw | 73-80 | 62-76 | 60-75 | 73-75 |
| Dc | 15.3-16 | 14-16 | 14-15.6 | 15.3-15.6 |

Table 16. Validation Experiments

| Experiment No. | Pon | Dw | Dc | Hole circularity at entry | Hole circularity at the exit | Hole taper |
|----------------|-----|----|------|---------------------------|------------------------------|------------|
| 1. | 9.5 | 73 | 15.3 | 0.775 | 0.701 | 0.012 |
| 2. | 9.6 | 74 | 15.4 | 0.790 | 0.700 | 0.014 |
| 3. | 9.7 | 75 | 15.5 | 0.807 | 0.700 | 0.017 |

the present work, it has been considered for analysis that the value of hole taper if less than 0.05 can be treated as trending to 0 or minimum value. Accordingly, the range of input parameters pertaining to hole taper less than 0 has been ascertained from the contour plots 11-13, as listed in Table 14. In Table 14 an intersection range for hole taper has also been evaluated by taking the intersection of obtained values from different plots. This intersection range pertains to hole taper less than 0.05. Moreover, after evaluating the suitable range for the quality characteristics, a final intersection range of input

calculated for these experiments as listed in Table 16. From the validation experiments, it has been found that the obtained range of input parameters is significant and the value of hole taper is reduced significantly.

Conclusion

After extensive experiential work on the fabrication of a high-strength aluminium-based metal matrix composite (MMC) with improved properties through the addition of SiC and Mg to AA2024 alloy, the following conclusive points have been derived:

- AA2024 alloy, commonly used in aerospace industries, can be significantly enhanced by incorporating SiC and Mg in educated proportions.
- The stir-casting process has proven to be an economically viable and suitable method for producing these hybrid composites.
- To achieve accurate drilling, Electric Discharge Machining (EDM) was adopted for the fabricated composite sheets.
- Utilizing Response Surface Methodology (RSM), mathematical models have been developed to optimize the response parameters for the machining process.
- Through thorough analysis, a specific range of input parameters critical for obtaining precise drilling results have been identified: Pon should be selected between 9.5 to 9.5, Dw between 73 to 75, and Dc between 15.3 to 15.6.
- The validation experiments conclusively demonstrated the significance of the identified input parameter range, confirming its efficacy in achieving desired results.

In the near future, the proposed methodology can be adopted for exploring other quality characteristics and diverse machining operations relevant to these composite materials. This research opens up promising avenues for further enhancing the performance and applications of high-strength aluminium-based metal matrix composites in the near future. The aerospace industry, in particular, stands to benefit from these advancements, fostering innovation and progress in this field.

Conflict of Interest

The authors declare no conflict of interest.

References

- Arora, P. K., Shrivastava, Y., & Kumar, H. (2023). Optimising FDM printing parameters for improved tensile properties in 3D printed ASTM D638 standard samples. *Australian Journal of Mechanical Engineering*, 1–14. <https://doi.org/10.1080/14484846.2023.2283663>
- Ferreira, S. L., Bruns, R. E., Ferreira, H. S., Matos, G. D., David, J. M., Brandão, G. C., Da Silva, E., Portugal, L. A., Reis, P. S. D., Souza, A. S., & Santos, W. N. L. D. (2007). Box-Behnken design: An alternative for the optimization of analytical methods. *Analytica Chimica Acta*, 597(2), 179–186. <https://doi.org/10.1016/j.aca.2007.07.011>
- Gudipudi, S., Selvaraj, N., Subbu, S. K., & Chilakalapalli, S. P. R. (2021). A comprehensive investigation on machining of composites by EDM for microfeatures and surface integrity. *Journal of Micromanufacturing*, 5(1), 5–20. <https://doi.org/10.1177/25165984211063308>
- Jain, A., & Singh, B. (2019a). Heat-Affected zone investigation during the laser beam drilling of hybrid composite using statistical approach. *Arabian Journal for Science and Engineering*, 45(2), 833–848. <https://doi.org/10.1007/s13369-019-04162-5>
- Jain, A., & Singh, B. (2019b). Analysis of heat affected zone (HAZ) during micro-drilling of a new hybrid composite. *Proceedings of the Institution of Mechanical Engineers, Part C: Journal of Mechanical Engineering Science*, 234(2), 620–634. <https://doi.org/10.1177/0954406219877911>
- Kumar, A., Grover, N., Manna, A., Kumar, R., Chohan, J. S., Singh, S., Singh, S., & Pruncu, C. I. (2021). Multi-Objective optimization of WEDM of aluminium hybrid composites using AHP and genetic algorithm. *Arabian Journal for Science and Engineering*, 47(7), 8031–8043. <https://doi.org/10.1007/s13369-021-05865-4>
- Kumar, H., Manna, A., & Kumar, R. (2018). Modeling and desirability approach-based multi-response optimization of WEDM parameters in machining of aluminium metal matrix composite. *Journal of the Brazilian Society of Mechanical Sciences and Engineering*, 40(9). <https://doi.org/10.1007/s40430-018-1368-1>
- Kumar, J., Singh, D., Kalsi, N. S., Sharma, S., Mia, M., Singh, J., Rahman, M. A., Khan, A. M., & Rao, K. V. (2021). Investigation on the mechanical, tribological, morphological and machinability behavior of stir-casted Al/SiC/Mo reinforced MMCs. *Journal of Materials Research and Technology*, 12, 930–946. <https://doi.org/10.1016/j.jmrt.2021.03.034>
- Lu, X., Yu, P., Li, W., Hayat, M. D., Yang, F., Singh, H., Song, W., Qu, X., Xu, Y., & Cao, P. (2020). High-performance Ti composites reinforced with in-situ TiC derived from pyrolysis of polycarbosilane. *Materials Science and Engineering: A*, 795, 139924. <https://doi.org/10.1016/j.msea.2020.139924>
- Mallick, A., Setti, S. G., & Sahu, R. K. (2023). Centrifugally cast functionally graded materials: Fabrication and challenges for probable automotive cylinder liner application. *Ceramics International*, 49(6), 8649–8682. <https://doi.org/10.1016/j.ceramint.2022.12.148>
- Myers, R. H., Montgomery, D. C., & Anderson-Cook, C. M. (2018). Response Surface Methodology: Process and Product Optimization Using Designed

- Experiments (Wiley Series in Probability and Statistics)," ed: Wiley, New York, 2009.
- Muni, R. N., Singh, J., Kumar, V., Sharma, S., Sudhakara, P., Aggarwal, V., & Rajkumar, S. (2022). Multiobjective optimization of EDM parameters for Rice Husk AsH/CU/MG-Reinforced Hybrid AL-0.7Fe-0.6SI-0.375CR-0.25ZN Metal Matrix Nanocomposites for Engineering Applications: Fabrication and Morphological Analysis. *Journal of Nanomaterials*, 2022, 1–15. <https://doi.org/10.1155/2022/2188705>
- Nath, S., & Madhu, U. (2021). Study of Densification Behavior of SiAlONs Using Dysprosium Containing Additive System. *International Journal of Experimental Research and Review*, 26, 16-34. <https://doi.org/10.52756/ijerr.2021.v26.002>
- Nayak, R. K., Pradhan, M. K., & Sahoo, A. K. (2022). *Machining of Nanocomposites*. <https://doi.org/10.1201/9781003107743>
- Ravikumar, M., Reddappa, H., & Suresh, R. (2018). Aluminium composites fabrication Technique and Effect of Improvement in their mechanical Properties – a review. *Materials Today: Proceedings*, 5(11), 23796–23805. <https://doi.org/10.1016/j.matpr.2018.10.171>
- Reddy, M. C., Rao, K. V., & Suresh, G. (2021). An experimental investigation and optimization of energy consumption and surface defects in wire cut electric discharge machining. *Journal of Alloys and Compounds*, 861, 158582. <https://doi.org/10.1016/j.jallcom.2020.158582>
- Sandhu, I. S., Maurya, S. K., & Manna, A. (2022). Investigation of electrochemical discharge machining process variables during μ - drilling on stir casted novel Zn/ (Ag+ Fe)-MMC for biomedical applications. *Advances in Materials and Processing Technologies*, 9(4), 1941–1959. <https://doi.org/10.1080/2374068x.2022.2139895>
- Santiago-Herrera, M., Ibáñez, J. M., Díez-Hernández, J., Tamayo-Ramos, J. A., Pabel, T., Kneißl, C., Alegre, J., Martel-Martín, S., & Rumbo, C. (2022). Comparative Life Cycle Assessment of Green Sand Casting and Low Pressure Die Casting for the production of self-cleaning AlMg3-TiO2 Metal Matrix Composite. *Ecological Indicators*, 144, 109442. <https://doi.org/10.1016/j.ecolind.2022.109442>
- Sharma, S., Goyal, A., Bharadwaj, P., Oza, A. D., & Pandey, A. (2023). Application of metal matrix composite fabricated by reinforcement materials – A review. *Materials Today: Proceedings*. <https://doi.org/10.1016/j.matpr.2023.02.287>
- Shrivastava, Y. (2018). Stable cutting zone prediction in computer numerical control turning based on empirical mode decomposition and artificial neural network approach. *Transactions of the Institute of Measurement and Control*, 41(1), 193–209. <https://doi.org/10.1177/0142331218757285>
- Shrivastava, Y., & Singh, B. (2021). Tool chatter prediction based on empirical mode decomposition and response surface methodology. *Measurement*, 173, 108585. <https://doi.org/10.1016/j.measurement.2020.108585>
- Thakur, S. S., Patel, B., Upadhyay, R. K., Bagal, D. K., & Barua, A. (2022). Machining characteristics of metal matrix composite in powder-mixed electrical discharge machining – A review. *Australian Journal of Mechanical Engineering*, 1–23. <https://doi.org/10.1080/14484846.2022.2030089>
- Teng, X. (2018). Investigation into micro machinability of Mg based metal matrix composites (MMCs) reinforced with nanoparticles," Newcastle University, 2018.
- Tsao, C. J., & Hocheng, H. (2004). Taguchi analysis of delamination associated with various drill bits in drilling of composite material. *International Journal of Machine Tools & Manufacture*, 44(10), 1085–1090. <https://doi.org/10.1016/j.ijmactools.2004.02.019>
- Wang, P., Eckert, J., Prashanth, K., Wu, M., Kaban, I., Xi, L., & Scudino, S. (2020). A review of particulate-reinforced aluminium matrix composites fabricated by selective laser melting. *Transactions of Nonferrous Metals Society of China*, 30(8), 2001–2034. [https://doi.org/10.1016/s1003-6326\(20\)65357-2](https://doi.org/10.1016/s1003-6326(20)65357-2)
- Yadav, P., Ranjan, A., Kumar, H., Mishra, A., & Yoon, J. (2021). A Contemporary Review of Aluminium MMC Developed through Stir-Casting Route. *Materials*, 14(21), 6386. <https://doi.org/10.3390/ma14216386>
- Zamani, S. M. M., Behdinin, K., Razfar, M. R., Haghshenas, D. F., & Mohandesi, J. A. (2021). Studying the effects of process parameters on the mechanical properties in friction stir welding of Al-SiC composite sheets. *The International Journal of Advanced Manufacturing Technology*, 113(11–12), 3629–3641. <https://doi.org/10.1007/s00170-021-06852-7>
- Zhu, J., Jiang, W., Li, G., Guan, F., Yu, Y., & Zhao, F. (2020). Microstructure and mechanical properties of

SiCnp/Al6082 aluminium matrix composites prepared by squeeze casting combined with stir casting. *Journal of Materials Processing*

Technology, 283, 116699.

<https://doi.org/10.1016/j.jmatprotec.2020.116699>

How to cite this Article:

Ankit Jain, Cheruku Sandesh Kumar and Yogesh Shrivastava (2023). An Effort for Identifying Suitable Machining Range During Drilling of a Novel Al-Based Composite Using Electric Discharge Machine. *International Journal of Experimental Research and Review*, 36, 327-346.

DOI : <https://doi.org/10.52756/ijerr.2023.v36.030>



This work is licensed under a Creative Commons Attribution-NonCommercial-NoDerivatives 4.0 International License.